Functional Materials 17, No.4 (2010)

Structural evolution of ZrO_2–Y_2O_3 xerogels under high hydrostatic pressure

O.A.Gorban, S.A.Sinyakina, Yu.O.Kulik*, T.A.Ryumshina, S.V.Gorban**, I.A.Danilenko, T.E.Konstantinova

O. Galkin Donetsk Institute of Physics and Engineering, National Academy of Sciences of Ukraine, 72 R.Luxemburg St., Donetsk, Ukraine
*I.Franko Lviv National University, 50 Drahomanova St., Lviv, Ukraine
**National University for Economics and Business, 31 Schorsa St., Donetsk, Ukraine

Received June 16, 2010

The structure changes in hydroxide nanopowder ZrO_2–3%Y_2O_3–xHO_n (n=1,2) system under high hydrostatic pressure have been studied using small-angle X-ray scattering and EPR spectroscopy. It has been demonstrated that the studied xerogels are characterized by multiple levels of spactial structure that can be described as mass fractals. It has been shown that fractal dimensionalities of these levels tend to equalization, so a gradual transition to a monofractal system takes place. The structural changes in xerogel under high hydrostatic pressure have been found to be of of non-monotonic character with an extremum at about 600 MPa.

Методами малоуглового рентгеновского рассеяния и ЭПР спектроскопии проведено исследование структурных изменений, происходящих в ксерогеле системы ZrO_2–3%Y_2O_3–xHO_n в условиях высокого гидростатического воздействия. Показано, что для исследуемых ксерогелей характерна множественность уровней пространственного строения, которые могут быть описаны как массовые фракталы. Наблюдается тенденция к выравниванию фрактальных размерностей этих уровней, то есть происходит постепенный переход к монофрактальной системе. Показано, что действие давления на структуру ксерогеля носит немонотонный характер с экстремумом 600 МПа.

1. Introduction

The modern material science pays great attention to the development of technologies of obtaining of oxide nanomaterials with functional properties being of importance in catalysis, photocatalysis, microelectronics, optics, biotechnology, medicine, polymer chemistry, etc. [1, 2]. Among the major characteristics controlling these features are the size, phase composition, morphological peculiarities of the particles, the nature of the particle interaction, the space distribution character of particles, the dispersity and the aggregation degree thereof. At the same time, the formation of physical and chemical properties and structural characteristics of oxide nanoparticles are affected essentially by the synthesis method, the nature of precursors and alloying constituents [3–5]. So, it was shown before that at the stage of xerogel formation, the different physical factors such as temperature, treatment by ultra-high frequencies (MW-drying), pulse magnetic field (PMF) provide an increased dispersity and reduced aggregation ability of synthesized zirconia nanopowders [6, 7]. Moreover, the influence of high hydrostatic pressure on the structural organization of the nanoparticulate oxide system is very interesting and important with respect to the purposeful aggregation of nanopowder materials. This work is devoted to the evolution of structural or-

ganization in ZrO_2–3 mol.%Y_2O_3–nH_2O xerogels under high hydrostatic pressure (HHP).

It is to note that the structure of zirconia-based systems is formed in the course of complex physical and chemical processes of the coagel → xerogel → amorphous hydroxide → oxide transformation. Thus, the study of the relation between the xerogel structural organization and the properties of oxide systems formed on its base is very interesting. The self-organization of nanoparticles occurs already at the early stages of the xerogel synthesis and the formed structures are random to some extent. Nevertheless, such systems are characterized by a certain hierarchical structure organization and the representation of random fractal can be used to describe the system geometry [8]. The fractal geometry makes it possible to take the random events into account, so it is often used to describe the structure of chemical systems [9].

2. Experimental

The nanopowders of ZrO_2–3%Y_2O_3–nH_2O hydroxide xerogel were synthesized by co-precipitation method according to nitrate technology using MW radiation at 2.45 GHz frequency and 500 W power. The xerogel was subjected to high hydrostatic pressure varied up to 1 GPa. The small-angle X-ray scattering (SAXS) method was used to study the structural organization of ZrO_2–3mol.%Y_2O_3–nH_2O xerogels. The SAXS spectra were measured using a DRON-3 diffractometer in CuKα-radiation monochromated by reflection from (111) plane of a perfect Ge single crystal. To reduce the parasitic scattering area of the monochromating single crystal, a special slit device was placed in front of the sample with the displacement possibility of ±4 mm normal to the incident beam. The background of air scattering was restricted by a slit device in front of the X-ray radiation detector. The use of perfect Ge single crystal and collimation system of the primary and scattered beam allowed us to make the measurements starting from the angles $\theta = 0.2–0.3°$. The 0.1 mm wide slit before the detector provides the space resolution of $\Delta 2\theta = 0.16°$. The scattering intensity was recorded in the point scanning mode (the angle step was 0.05°, the exposure time 100 s). As at the smallest angles of scattering (0.2–0.4°), the scattered beam is superimposed with the primary radiation beam attenuated due to absorption within the sample, the primary beam intensity taking into account the absorption within the sample was subtracted from the measured intensity:

$$I(2\theta) = I_{exp.}(2\theta) - KI_0(2\theta)/\cos(2\theta), \quad (1)$$

where $I_0(2\theta)$ is the primary beam intensity distribution; $I_{exp.}(2\theta)$, the experimentally measured scattering intensity; $1/\cos(2\theta)$, the factor accounting the the beam path within the sample depending on the scattering angle. The absorption coefficient was calculated as

$$K = I(0)/I_0(0), \quad (2)$$

where $I_0(0)$, $I(0)$ are the intensities of the primary and the secondary beams at the detector position $2\theta = 0°$. The intensity was recorded within the s range from 0.1 to 2.55 nm^{-1}. The collimation correction was introduced according to the procedure in [10]. The experimental spectra were processed using the GNOM software [11].

The fractal dimension of the scattering area D_f was defined in the known way [12] from the slope of the corresponding linear section of the SAXS scattering curve presented in $\lg(I(s))$–$\lg(s)$ coordinates. To evaluate the space structure of the scattering xerogel area, the SAXS curves were analyzed in Kratky coordinates $I \cdot s^2$–s [13].

The EPR studies of xerogels were carried out using a standard PS-100X radiospectrometer with high-frequency modulation at 9 GHz and at room temperature. The MW power was chosen to be far from the saturation of the studied lines. The fifth CTC line of two-valent manganese ion in cubic manganese oxide for a calibrated sample was chosen as a reference mark of paramagnetic center concentration (PMC) The total intensity of the studied spectral lines was determined as the ratio of areas under the absorption curves for the samples and the reference mark line calculated using the double integration of the derivatives of absorption lines. The measurement relative error of the PMC content did not exceed 20 %.

3. Results and discussion

The xerogel structure can be presented as a solid frame consisting of mono-dispersed particles with a developed hydrate shell supplemented with porous space formed in the course of drying. Fig. 1 presents the SAXS profiles in $\lg(I(s))$–$\lg(s)$ coordinates for xerogels treated by hydro-

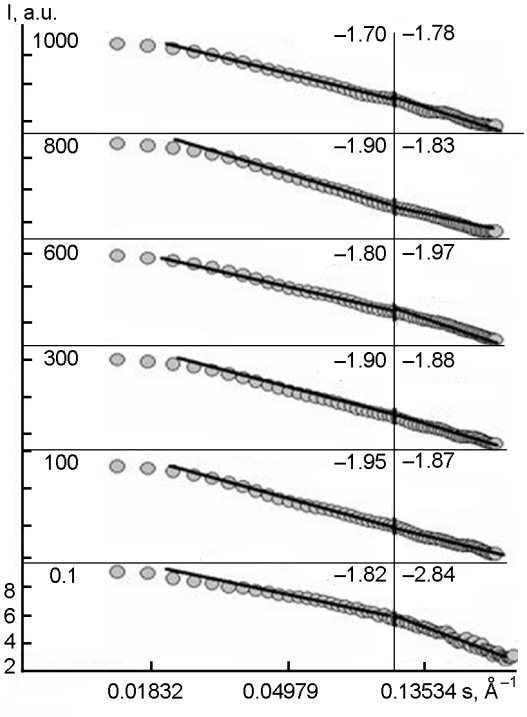

Fig. 1. Scattering data in Porod coordinates for ZrO_2–3%Y_2O_3–xOH_n xerogels subjected to high hydrostatic pressure.

static pressure of 300, 600, 800, 1000 MPa. The SAXS curve of the starting non-compressed powder is added, too.

The analysis of SAXS spectra for the starting ZrO_2–3%Y_2O_3–nH_2O xerogel testifies the multiple levels of the scattering area space structure: the curve in lg($I(s)$)–lg(s) coordinates consists of two parts differing in the angular dependence character of the radiation intensity on the wave vector s. The first part is associated with the scattering coordinate s values from 0.26 to 0.128 Å^{-1}, or in the direct space resolution $L = 2\cdot\pi/s$ from 2.4 to 5 nm. The second part has s values from 0.02 to 0.124 Å^{-1}, or in the direct space resolution $R = 2\pi/s$ from 25 to 5 nm. The fractal dimensionalities estimated at scale levels less than 5 nm and in the 5–25 nm range permit us to interprete them as a mass fractal with dimensionalities of 2.54 and 1.84, respectively.

The study of the xerogel structural organization evolution at varying applied pressure has shown that the high hydrostatic pressure (HHP) treatment at 100–1000 MPa results in the change of fractal dimensionality at all scale levels. The analysis of small-angle scattering spectra in logarithmical coordinates has demonstrated that in hydroxide system, within the applied range of pressures, the multiple levels of the scattering area space structure is retained with conservation of the fractal type. They all are described as a mass fractal. Moreover, non-monotonic evolution behavior of the hydroxide system fractal dimensionality is observed in dependence on the applied pressure value at all the scale levels.

The effect of pressure on the hydroxide structure at scale levels below 5–6 nm results in an essential "loosening" of the fractal structure demonstrated as the fractal dimensionality reduction from 2.54 for non-compressed hydroxide system down to 1.87, 1.88, 1.97, 1.83, and 1.78 for pressures of 100, 300, 600, 800, and 1000 MPa, respectively. As seen from the presented data, the pressure of 600 MPa exerts the least influence on the structural elements of hydroxide system at this scale level. At the same time, the hydrostatic compression of xerogel at 100, 300, and 800 MPa results in consolidation of the scattering area fractal structure at scale level above 5–6 nm (the estimated fractal dimensionalities are 1.95, 1.90 and 1.90, respectively). The systems compressed at 600 and 1000 MPa do not demonstrate such effect. The fractal dimensionality of hydroxide compressed is 1.80 at 600 MPa and 1.70 at 1000 MPa.

The comparison of fractal dimensionalities of hydrostatically compressed xerogel structures at the scale levels below 5–6 nm and above 6 nm has shown that fractal dimensionalities of those levels tend to equalization, thus, a gradual transfer to a monofractal system takes place. An exception is the xerogel compressed at 600 MPa where the "loosening" of fractal areas is observed at both scale levels. The fractal dimensionalities are 1.97 and 1.80 for scale levels below 5–6 nm and above 6 nm, respectively (to compare, those are 2.54 and 1.84 for non-compressed xerogel).

In order to estimate the space structure of the xerogel scattering area, the curves of small-angle X-ray scattering were analyzed using Kratky coordinates $I\cdot s^2$–s. The studied xerogel SAXS spectra in Kratky coordinates are presented in Fig. 2.

It is to note that in these coordinates, the scattering curve shape for the non-compressed xerogel answers to scattering from an object containing scattering fragments (pores and particles) with various characteristic sizes. It is seen that the treatment of xerogel with high hydrostatic pressure results in reduction of the total scattering capacity.

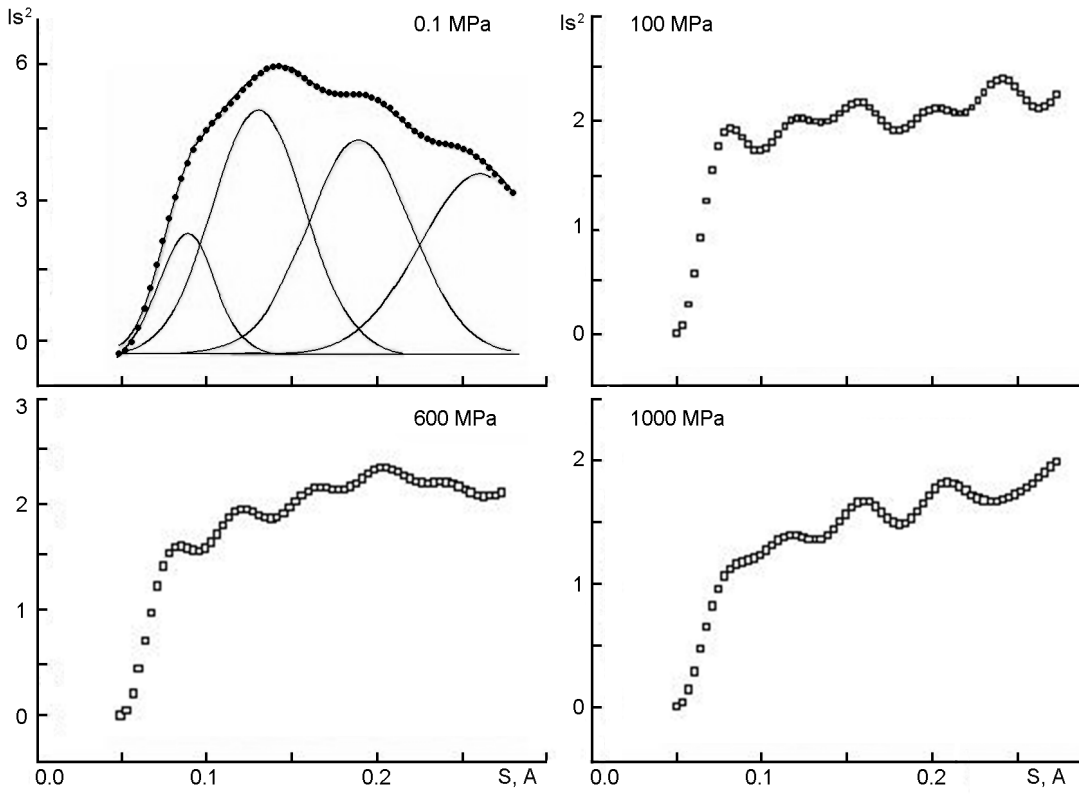

Fig. 2. SAXS intensity as a function of wave vector in Kratky coordinates.

The approximation of small-angle scattering experimental spectrum in Kratky coordinates using Gaussians made it possible to estimate characteristic sizes of scattering areas in the investigated systems, $L = 2 \cdot \pi / s$ (the approximation correlation coefficient is at least 0.999 for all the spectra). Table presents contributions from different structure fragments to the total scattering capacity of the studied systems and characteristic sizes of the scattering areas.

It is seen that that for the non-compressed xerogel, a considerable fraction of the total scattering capacity is contributed by the scattering on fragments with the average characteristic sizes of 7 and 3 nm. Before [17], it was revealed by transmission electron microscopy that the average particle size in the ZrO_2–3%Y_2O_3–nH_2O hydroxide system is about 3–5 nm. This fact allows us to interprete the scattering from the areas of 3–4 nm characteristic size as the scattering on monodispersed hydroxide particles forming the xerogel skeleton. However, the pores of the same size may contribute to the scattering in this area, too. Most probably, the scattering areas of 16–23 nm size can be associated with the aggregates of xerogel particles. The exposure of xerogel to high hydrostatic pressure results in the reduction of total scattering capacity. The average scattering fragment

Table. Characteristic sizes of scattering areas.

Pressure, MPa	Scattering area size, nm (contribution to the total scattering, %)				
0.1	16(9)	7(45)		4(5)	3(40)
100	23(17)	9(26)	6(17)	4(9)	3(32)
300	23(14)	10(23)	6(23)	4(9)	3(30)
600	23(14)	9(25)	6(10)	4(7)	3(44)
800	21(13)	10(19)	5(39)	3(15)	3(13)
1000	23(9)	10(18)	6(8)	4(8)	2(57)

size increases up to 23 nm in the areas with small s, so the fraction of their contribution to the total scattering capacity rises, too. This testifies a change of the system aggregation state.

As to the scattering area of 7 nm average size, it must be most probably identified as a pore, too. It is seen from Table that all xerogels compressed at the studied pressure values demonstrated the disappearance of 7 nm scattering area (this area makes the main contribution to the total scattering capacity of the non-compressed hydroxide) while the areas of 5–6 nm and 9–10 nm emerge in the structure. Note that the contributions from the 5–6 and 9–10 nm areas for compressed hydroxides correspond to the contribution from 7 nm area for non-compressed xerogel. The sizes of these areas do not depend on the pressure value applied to the xerogel.

Let us consider the xerogel as an inhomogeneous structure containing open and closed pores containing adsorbed water bound with the hard framework. The bound water can be treated as the second phase rigidly bound with the solid ZrO_2 phase. The estimations show that the pressure inside the pores calculated on the formula

$$p = \frac{4\gamma}{D}\cos\theta, \qquad (3)$$

where D is the pore diameter; γ, the surface tension coefficient of water; θ, the wetting angle of the surface, is $p \approx -2.2 \cdot 10^7$ Pa at 2 nm pore diameter, and $p \approx -0.41 \cdot 10^7$ Pa at 10.6 nm. It is seen that the pressure inside the pores is 1–2 orders lower than the applied external hydrostatic pressure, so it plays an insignificant role at high pressures. The main effect is due to the external applied pressure and it acts in two ways. For the upper scale levels with the size above 5 nm, the influence of relatively low pressures of 100–300 MPa results in rapprochement of powder particles to the distances where the external hydroxile groups become able to interact and to connect the particles into a single agglomerate without violating the inner structure. In this case, the pressed material density is reduced due to formation of new closed pores and former open ones. As the pressure increases, its second aspect begins to reveal itself associated with the increase of additional boundary "misfit" stresses. Being coordinated by the solid phase, the water within small closed pores has a compressibility which differs by several orders from that of the solid phase. Due to the essential difference in the compressibilities of the phases under HGP, shear misfit stresses arise at zirconia/water phase interfaces. It is shown in [14] that the magnitude of these stresses depends both on the pressure value and the compressibility difference between the phases γ_1, γ_2 according to expression

$$\sigma_v = \frac{\gamma_1 - \gamma_2}{\gamma_1 + \gamma_2} p, \qquad (4)$$

where p is pressure; γ_1 and γ_2, compressibilities of phases: for water, $\gamma_1 = 0.125 \cdot 10^{-9}$ Pa^{-1}, for ZrO_2, $\gamma_2 = 0.0054 \cdot 10^{-9}$ Pa^{-1} [15]. The estimation of misfit stresses according to (4) shows that the stress increases from 92 MPa under 100 MPa pressure to 920 MPa at 1000 MPa. The additional shear "misfit" stress value is rather high and able to break the interphase bonds and squeeze out water from pores, that results both in increased material density and the breaking of the material at the low scale level. The action of two trends defines the sudden change in the properties near 600 MPa.

The EPR studies of xerogels dried at 140°C have shown that an isotropic signal with g-factor of 2.003 is registered in EPR spectra of samples treated by high hydrostatic pressure. This signal is usually associated with the appearance of F center due to removal of water molecule and OH groups from the particle surface [16]. Note that the non-compressed xerogel dried in the same conditions does not have paramagnetic centers. So, xerogels compressed at 100, 600, 800, and 1000 MPa show the paramagnetic center concentrations of $4.38 \cdot 10^{13}$, $9.27 \cdot 10^{12}$, $2.35 \cdot 10^{13}$, and $1.75 \cdot 10^{13}$ spin/mg. A good agreement is observed between the evaluated concentrations of the registered oxygen vacancies in dried compressed xerogels and the evaluated misfit stresses. The variation of paramagnetic centers concentration depending on the pressure according to EPR spectra testifies an extremum near 600 MPa, too. This may be due be also to the realization of two trends in the pressure influence.

Thus, the structure of the initial xerogel contains the scattering fragments (pores and particles) with various characteristic sizes. It is shown that the evolution of the

zirconia nanoparticular system occurs under high hydrostatic pressure. At the scale level below 5–6 nm and above 6 nm, the comparison of structure fractal dimensionalities in hydrostatically compressed xerogels has shown that the fractal dimensionalities of this levels tend to equalization, so a gradual transition to a monofractal system takes place.

4. Conclusions

The structural organization evolution in ZrO_2–3%Y_2O_3–xOH_n xerogels has been studied. It has been shown that the studied xerogels are characterized by the multiple levels of space structure that can be described as mass fractals. It has been found that in the systems exposed to HGP, fractal dimensionalities of these levels tend to equalization, so a gradual transition to a monofractal system takes place. The characteristic sizes of the scattering areas of the studied systems have been estimated and it is shown that the systems exposed to HGP lose the scattering fragments of 7 nm size while the areas of 5–6 and 9–10 nm size appear in the structure. The contributions from those 5–6 and 9–10 nm areas to the total scattering intensity correspond to that from the 7 nm one. The additional interface misfit stresses of shear character are estimated in the small pores.

References

1. T.E.Konstantinova, I.A.Danilenko, N.P.Pilipenko et al., Electrochemical Society Proceedings, Paris, France, 2003-07, 153 (2003).
2. Xin-Mei Liu, G.Q.Lu, Zi-Feng Yan, *Appl. Catalysis A:General.*, **279**, 241 (2005).
3. W.T.M.Croot Zevert, A.I.A.Winnubst, G.S.A.M. Theunissen, A.I.Burggraat, *J. Mater. Sci.*, **25**, 3449 (1990).
4. A.G.Belous, E.V.Pashkova, A.N.Makarenko, *Nanosystems, Nanomaterials, Nanotechnologies*, **1**, 85 (2003).
5. Chuanyong Huang, Zilong Tang, Zhongtai Zhang, *J.Am.Ceram.Soc.*, **84**, 1637 (2001).
6. N.P.Pilipenko, Y.A.Danilenko, T.E.Konstantinova et al., *Functional Materials*, **5**, 221 (1998).
7. N.P.Pilipenko, T.E.Konstantinova, V.V.Tokiy et al., *Functional Materials*, **9**, 545 (2002).
8. A.I.Olemskoi, A.Ya.Flat, *Usp.Fiz.Nauk*, **163**, 1 (1993).
9. D.Shefer, K.Kefer, in: Proc. of 6th Int. Symp. on Fractals in Physics, Triest, Italy (1985).
10. B.V.Schedrin, L.A.Feigin, *Kristallografia*, **11**, 159 (1966).
11. D.I.Svergun, A.V.Semenyak, L.A.Feigen, *Acta Cryst.*, **A44**, 244 (1988).
12. J.E.Marin, A.J.Hurd, *J.Appl.Cryst.*, **20**, 61 (1987).
13. G.Porod, *Kolloid Z.*, **51**, 109 (1952).
14. T.A.Ryumshina, *Ukr.Fiz.Zh.*, **31**, 581 (1986).
15. Tables of Physical Quantities: A Reference Book, ed. by N.K.Kikoin, Atomizdat, Moscow (1976) [in Russian].
16. I.V.Bobrischeva, I.A.Stavitsky, V.K.Yermolaev et al., *Catal.Lett.*, **56**, 23 (1998).

Структурна еволюція ксерогелів ZrO_2–Y_2O_3 в умовах високого гідростатичного тиску

О.О.Горбань, С.А.Синякіна, Ю.О.Кулик, Т.А.Рюмшина, С.В.Горбань, І.А.Даниленко, Т.Є.Константінова

Методом малокутового рентгенівського розсіювання та ЕПР спектроскопії проведено дослідження структурних змін у ксерогелі системи ZrO_2–3%Y_2O_3–nH_2O в умовах високого гідростатичного тиску. Показано, що для ксерогелей, що досліджено, спостерігається множинність рівнів просторової структури, які можуть бути описані як масові фрактали. Спостерігається тенденція до вирівнювання фрактальних розмірностей цих рівнів, тобто відбувається поступовий перехід до монофрактальної структури. Показано, що дія тиску на структуру ксерогелю має немонотонний характер з екстремумом біля 600 МПа.